Elevated Glucose Represses Liver Glucokinase and Induces Its Regulatory Protein to Safeguard Hepatic Phosphate Homeostasis

Catherine Arden,[1] John L. Petrie,[1] Susan J. Tudhope,[1] Ziad Al-Oanzi,[1,2] Amy J. Claydon,[3] Robert J. Beynon,[3] Howard C. Towle,[4] and Loranne Agius[1]

OBJECTIVE—The induction of hepatic glucose 6-phosphatase (G6pc) by glucose presents a paradox of glucose-induced glucose intolerance. We tested whether glucose regulation of liver gene expression is geared toward intracellular homeostasis.

RESEARCH DESIGN AND METHODS—The effect of glucose-induced accumulation of phosphorylated intermediates on expression of glucokinase (Gck) and its regulator Gckr was determined in hepatocytes. Cell ATP and uric acid production were measured as indices of cell phosphate homeostasis.

RESULTS—Accumulation of phosphorylated intermediates in hepatocytes incubated at elevated glucose induced rapid and inverse changes in Gck (repression) and Gckr (induction) mRNA concomitantly with induction of G6pc, but had slower effects on the Gckr-to-Gck protein ratio. Dynamic metabolic labeling in mice and liver proteome analysis confirmed that Gckr and Gck are low-turnover proteins. Involvement of Max-like protein X in glucose-mediated Gck-repression was confirmed by chromatin immunoprecipitation analysis. Elevation of the Gck-to-Gckr ratio in hepatocytes was associated with glucose-dependent ATP depletion and elevated urate production confirming compromised phosphate homeostasis.

CONCLUSIONS—The lowering by glucose of the Gck-to-Gckr ratio provides a potential explanation for the impaired hepatic glucose uptake in diabetes. Elevated uric acid production at an elevated Gck-to-Gckr ratio supports a role for glucose regulation of gene expression in hepatic phosphate homeostasis. ***Diabetes*** **60:3110–3120, 2011**

Glucokinase (Gck) catalyses the first reaction in hepatic glucose metabolism and has a major role in the control of hepatic glucose disposal and thereby of blood glucose homeostasis. Its activity is regulated by an inhibitory protein, Gckr, that sequesters Gck in the nucleus during fasting and enables dissociation of Gck and translocation to the cytoplasm in response to elevated blood glucose after a meal (1). The rate of glucose phosphorylation is dependent on rapid adaptive regulation involving dissocation of Gck from the sequestered Gckr pool but also on small fractional changes in the concentrations of Gck and Gckr, as shown by the unusually high control strength of these proteins on glucose metabolism (2–4). Consistent with the major role for Gck in control of blood glucose homeostasis, transcription of the Gck gene in the liver is induced by insulin and repressed by glucagon (5). Type 2 diabetes is associated with defects in hepatic glucose uptake and production (6–10), and a role for defective Gck regulation or expression has been implicated (8–10); however the underlying mechanisms are unresolved.

Liver Gck is a major determinant of the hepatic concentration of glucose 6-P, which is a linear function of the free Gck activity (1). Conversely, glucose 6-phosphatase (G6pc) is a major negative regulator of the hepatic glucose 6-P concentration (11,12). Several studies have shown that high glucose concentration causes transcriptional activation of G6pc (13–17) concomitantly with induction of glycolytic and lipogenic genes (17). The latter is conventionally rationalized as an adaptive mechanism to convert dietary glucose to triglyceride for energy storage (17). Accordingly, induction of G6pc, which promotes enhanced glucose production, is generally viewed as a paradoxical response to glucose (18). Various hypotheses have been proposed to explain the possible adaptive advantage of the glucose induction of G6pc in relation to blood glucose homeostasis (18,19). However, overexpression of G6pc causes glucose intolerance (20), which argues against an adaptive role for G6pc induction in blood glucose homeostasis. An alternative hypothesis is that glucose induction of G6pc is a mechanism to maintain intracellular homeostasis of phosphorylated intermediates as opposed to extracellular glucose. This hypothesis predicts that high glucose concentration would repress genes that promote expansion of the phosphometabolite pool (Gck, Pck1) concomitantly with induction of G6pc and Pklr (Fig. 1). This study provides evidence in support of this hypothesis.

RESEARCH DESIGN AND METHODS

Reagents. S4048 (21) was a gift from Dr. D. Schmoll, Aventis, Pharma-GmbH, Frankfurt, Germany.

Hepatocyte culture and treatment with adenoviral vectors. Hepatocytes were isolated from male Wistar rats fed ad libitum (4), obtained from Bantin & Kingman, Hull, U.K., or from Harlan, Bicester, U.K. Procedures conformed to Home Office regulations and were approved by the local ethics committee. Hepatocytes were suspended in minimum essential medium (MEM) supplemented with neonatal calf serum (5% v/v) and seeded on gelatin-coated (1 mg/mL) multiwell plates. After cell attachment (4 h), the medium was replaced by serum-free MEM containing 5 mmol/L glucose and 10 nmol/L dexamethasone, and the hepatocytes were cultured for 18 h. Treatment with adenoviral vectors was in serum-free MEM between 2 and 4 h after cell attachment. Adenoviral vectors for Gck, Gckr, wild-type (WT) Max-like protein (Mlx) (Mlx-WT), dominant-negative (DN) Mlx (Mlx-DN), carbohydrate response element binding protein (ChREBP)-WT, and ChREBP-DN were described previously (4,17).

From the [1]Institute of Cellular Medicine, Newcastle University, Newcastle upon Tyne, U.K.; the [2]Department of Laboratory Medicine, Al-Jouf University, Sakaka, Saudi Arabia; the [3]Protein Function Group, Institute of Integrative Biology, University of Liverpool, Liverpool, U.K.; and the [4]Department of Biochemistry, Molecular Biology and Biophysics, University of Minnesota, Minneapolis, Minnesota.

Corresponding author: Loranne Agius, Loranne.Agius@ncl.ac.uk.

Received 19 January 2011 and accepted 18 September 2011.

DOI: 10.2337/db11-0061

This article contains Supplementary Data online at http://diabetes.diabetesjournals.org/lookup/suppl/doi:10.2337/db11-0061/-/DC1.

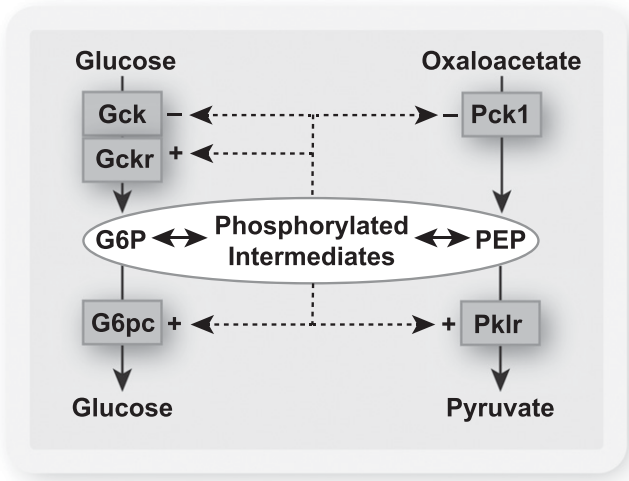

FIG. 1. Hypothesis: glucose-regulated gene expression in the liver is a mechanism for intracellular homeostasis of phosphorylated intermediates. When the hepatocyte is challenged with elevated glucose, the increase in the concentrations of phosphorylated intermediates represses enzymes that catalyze the entry of substrate into the phosphometabolite pool (Gck and Pck1) and induces enzymes (G6pc and Pklr) that catalyze depletion of phosphorylated intermediates. Gckr is the inhibitor protein of Gck.

Incubations with substrates. Incubations for substrate-regulated gene expression were performed after preculture of the hepatocytes for 18 h in fresh MEM containing 10 nmol/L dexamethasone, 10 nmol/L insulin, 5 mmol/L glucose (unless otherwise indicated), and the additions indicated. Parallel incubations were performed for RNA extraction and metabolite determination. mRNA decay was determined as described by Iynedjian et al. (22). Glucose phosphorylation was determined from the metabolism of [2-^{3}H]glucose (4).

Metabolites, enzyme activity, and immunoactivity. For cell metabolite determination, the medium was drained and the plates were snap-frozen in liquid nitrogen. The cells were extracted in 10% w/v perchloric acid, and the deproteinized supernatant was neutralized with 3M K_2CO_3. ATP was determined with a luciferase assay kit (FL-AA; Sigma-Aldrich, St. Louis, MO), and glucose 6-P was determined fluorimetrically (Ex 530 nm, Em 590 nm, Spectramax, Me5) by coupling NAD(P)H formation to reduction of resazurin with diaphorase (23). Uric acid accumulation in the medium was determined by a colorimetric method involving reduction of ferric ion coupled to formation of ferrous-tripyridyltriazine complex (24) and by a uricase-peroxidase assay coupled to *N*-acetyl-3,7-dihydroxyphenoxazine conversion to resorufin (25). Gck enzyme activity was determined as described previously (4). Immunoactivity was determined by Western blotting. Hepatocyte extract (20 μg protein) was fractionated by SDS-PAGE and transferred to nitrocellulose. Membranes were incubated overnight with antibodies against Akt-S473-P, Akt total (Cell Signaling #9271, #9272), Gck, and Gckr (gifts from AstraZeneca) and then for 1 h with horseradish peroxidase–labeled anti-rabbit IgG (Dako), and immunoreactive bands were visualized by enhanced chemiluminescence and quantified by densitometry.

Protein turnover in vivo. Twenty-five hybrid (BALB/c × S57BL6/J, F1) male laboratory mice provided all tissue samples. They were housed individually in 12-h light:dark reverse lighting. Two diets based on the 5002 Certified Rodent Diet (LabDiet; Purina Mills, PMI, Richmond) were used, both containing an equivalent quantity of valine (1.05%) as either unlabeled or [$^2H_8$]valine. Mice were acclimated to the unlabeled diet and monitored to assess food intake prior to the labeling phase. The mice were then fed the [$^2H_8$]valine-containing diet at a nominal relative isotope abundance of 0.5 for up to 35 days. Pairs of animals were killed at the intervals indicated, and liver proteins were extracted (26), reduced with dithiothreitol (3 mmol/L, 10 min, 60°C) alkylated with iodoacetamide (9 mmol/L, 30 min), and trypsin digested (0.01 μg/μL, 16 h, 37°C). The surfactant was inactivated and precipitated with trifluoroacetic acid (0.5% v/v, 45 min, 37°C) and clarified by centrifugation (13,000*g*, 15 min). Digests (500 ng protein) were analyzed on a Thermo LTQ-Orbitrap Velos system using a 75 μm × 150 mm BEH C18 column, and the peptides were resolved over a linear organic gradient of 3–40% acetonitrile in 0.1% v/v formic acid. Data acquisition was in data-dependent mode, with the top 20 most intense peptides in each mass spectrometry scan selected for fragmentation (26). The raw data collected were processed using default parameters in Proteome Discoverer and the mgf file created was searched against the UniProt *Mus* database using Mascot (v. 2.3.01).

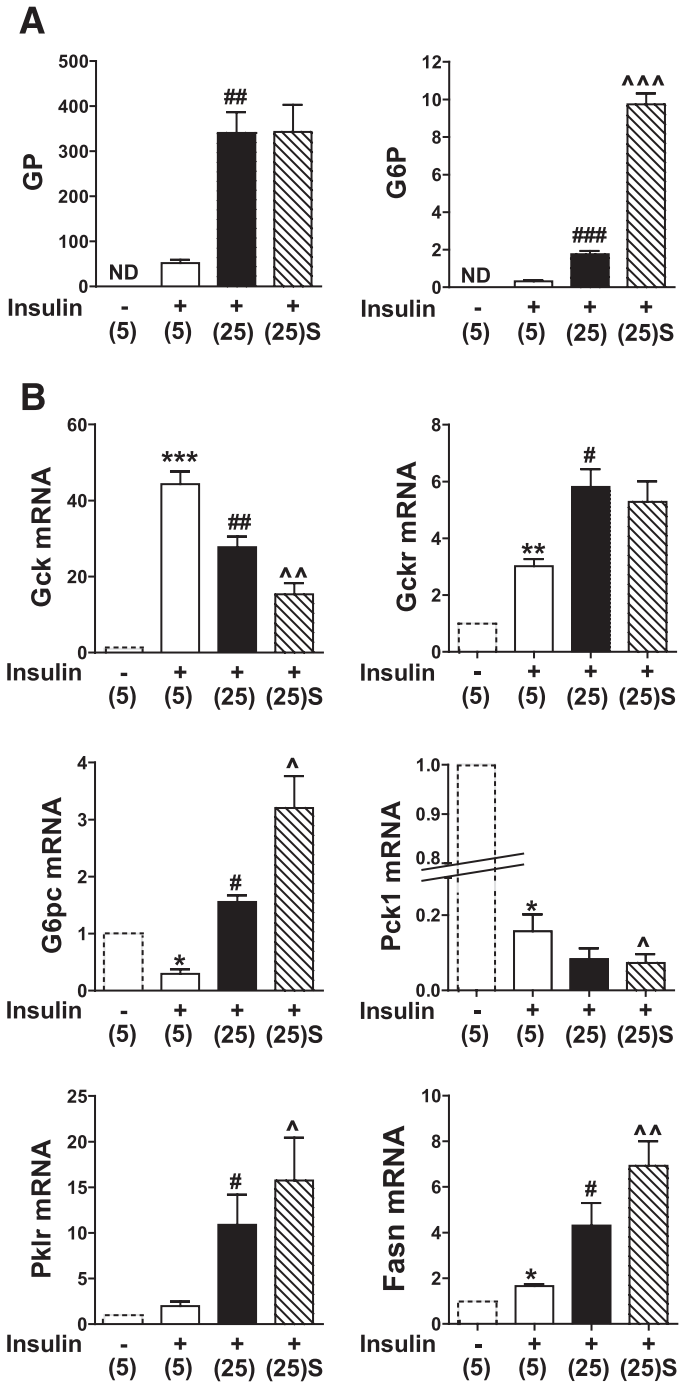

FIG. 2. Glucose represses Gck expression concomitantly with induction of G6pc and Pklr. Hepatocytes were precultured for 18 h in medium containing 5 mmol/L glucose and then incubated for 4 h in fresh MEM without (hatched line) or with 10 nmol/L insulin and 5 mmol/L (5) or 25 mmol/L glucose (25) without or with 2 μmol/L S4048 [(25)S]. *A*: Glucose phosphorylation (GP, nmol/h mg protein) and glucose 6-P (G6P, nmol/mg protein). *B*: mRNA levels of the target genes indicated expressed relative to 5 mmol/L glucose without insulin (first bar). Means ± SEM, n = 3–6. *P < 0.05, **P < 0.01, ***P < 0.005, effect of insulin; #P < 0.05, ##P < 0.01, ###P < 0.005, effect of substrate; ^P < 0.05, ^^P < 0.01, ^^^P < 0.005, effect of S4048. ND, not determined.

Real-time RT-PCR. RNA was extracted in TRIzol (Invitrogen) (27), and cDNA was synthesized from 1 μg of RNA with random hexamers and Superscript (Invitrogen). Sybr-Green–based real-time RT-PCR was performed in a volume of 10 μL containing 50 ng of reverse-transcribed RNA and 5 ng of forward and

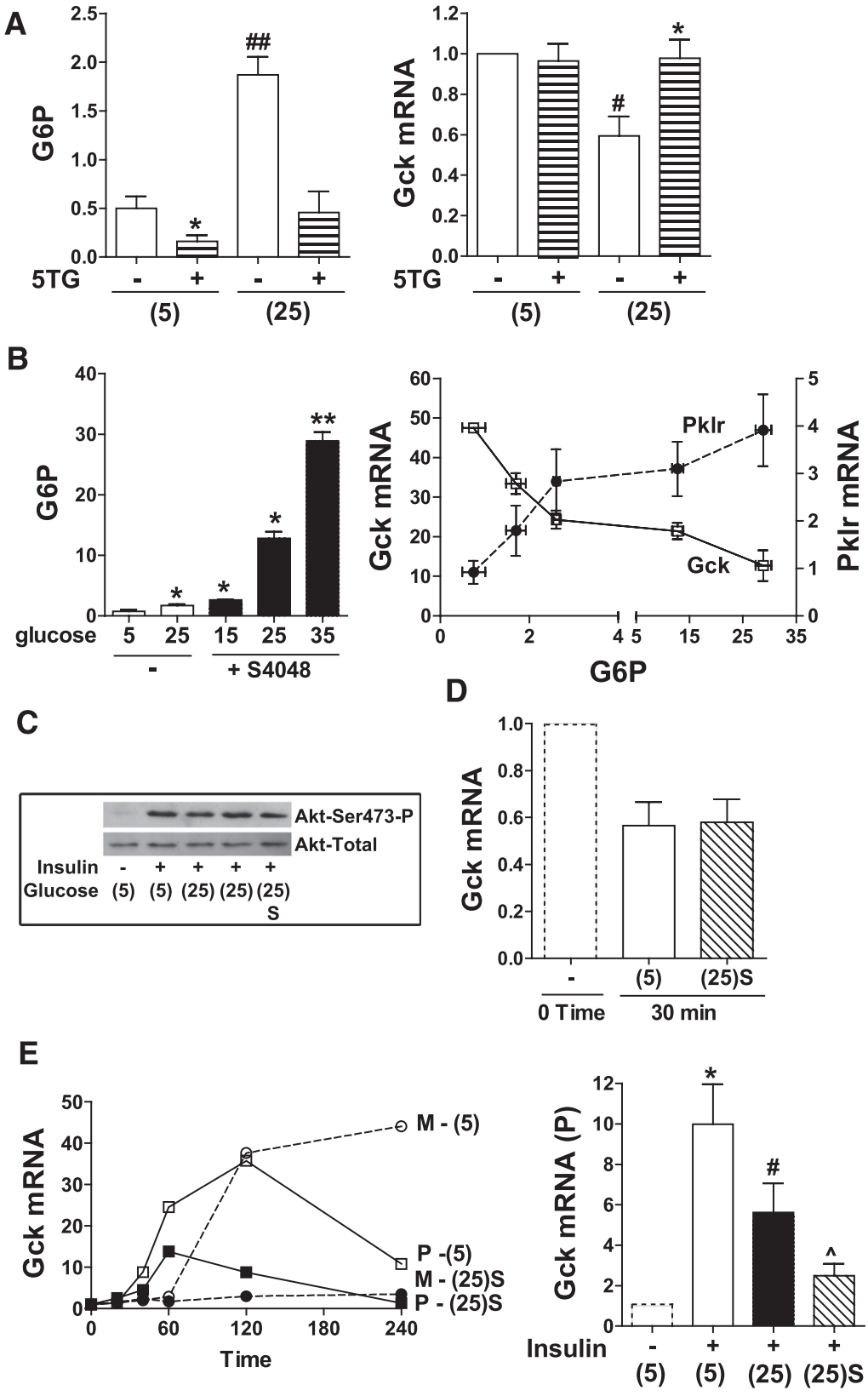

FIG. 3. Glucose metabolites repress Gck expression. *A*: Hepatocytes were incubated for 4 h with 10 nmol/L insulin at 5 mmol/L (5) or 25 mmol/L glucose (25) −/+ 3 mmol/L 5-thioglucose (5TG) for determination of glucose 6-P (G6P, nmol/mg protein) and Gck mRNA (expressed relative to 5 mmol/L glucose). Means ± SEM, $n = 3$. *$P < 0.05$, effect of 5-thioglucose; #$P < 0.05$, ##$P < 0.01$, effect of 25 mmol/L glucose. *B*: Hepatocytes were incubated for 4 h with 10 nmol/L insulin and glucose (5, 15, or 35 mmol/L) without (open bars) or with 2 μmol/L S4048 (filled bars) for determination of glucose 6-P (nmol/mg protein) and Gck and Pklr mRNA plotted against the respective glucose 6-P. $n = 3$. *$P < 0.05$, **$P < 0.01$. *C*: Hepatocytes were incubated for 1 h with the additions indicated [5 mmol/L (5) or 25 mmol/L glucose (25) or 25 mmol/L glucose + S4048 (25)S]. Immunoblots to Akt-S473-P and total-Akt, representative of two experiments. *D*: Hepatocytes were preincubated for 4 h with 10 nmol/L insulin. Gck mRNA decay was determined as described in the RESEARCH DESIGN AND METHODS with 5 mmol/L or 25 mmol/L glucose + S4048 [(25)S]. mRNA levels are expressed relative to time 0. Means ± SEM, $n = 4$. *E*:

reverse primers (Supplementary Table 1) in a Roche Capillary Light Cycler, with initial denaturation at 95°C for 10 min followed by 40–50 cycles of 95°C for 15s, 58°C for 7s, and 72°C for 15s. Relative mRNA levels were calculated by the Δ cycle threshold method using as reference the RNA from the respective control at 5 mmol/L glucose. Δ Cycle threshold values for cyclophilin tested as a negative control were negligible for all substrate conditions tested.

Chromatin immunoprecipitation. Hepatocytes in 150 cm^2 dishes were incubated for 4 h with substrates, and the incubations were terminated with formaldehyde (1% v/v, 10 min, 37°C) followed by glycine (0.125 M, 5 min) to terminate cross-linking. Chromatin immunoprecipitation (ChIP) assays were performed using the Upstate Biotechnology ChIP assay kit (#17–295; Millipore, Billerica, MA). Cells were washed in PBS, pelleted, and suspended in 3 mL lysis buffer (1% SDS, 10 mmol/L EDTA, 50 mmol/L Tris, pH 8.1) and sonicated to give sheared DNA fragments between 100 and 1,000 bp. They were centrifuged (13,000*g*, 10 min, 4°C), and 500 μL lysate was diluted 10-fold in ChIP dilution buffer (0.01% SDS, 1.1% Triton X-100, 1.2 mmol/L EDTA, 16.7 mmol/L Tris-HCl, pH 8.1, 167 mmol/L NaCl). Supernatants were precleared with 75-μL protein A agarose/salmon sperm DNA (50% slurry), and cell supernatants were incubated overnight (4°C) with 6 μg IgG against ChREBP (NB400–135; Novus Biologicals, Littleton, CO), Mlx, or control IgG (sc-2027, sc-14705; Santa Cruz Biotechnology, Santa Cruz, CA). Immune complexes were collected by incubation with 120 μL protein A agarose/salmon sperm DNA (ChREBP, IgG) or 120 μL protein G agarose/salmon perm DNA (Mlx) for 3h at 4°C. Agarose pellets were washed with low salt (#20–154), high salt (20–155), LiCl (#20–156), and TE (#20–157) wash buffers for 5 min each with rotation at 4°C. Immune complexes were eluted by addition of elution buffer (1% SDS, 0.1M $NaHCO_3$) for 30 min with rotation at room temperature, and cross-links were reversed by addition of 5 M NaCl and heating at 65°C for 4 h. Samples were then incubated with 0.5 M EDTA, 1 M Tris-HCl, pH 6.5, and Proteinase K (P4850; Sigma, St. Louis, MO) for 1 h at 45°C. DNA was recovered by phenol/chloroform extraction and amplified by Touchdown real-time PCR with primer sequences amplifying promoter regions of the Pklr and Gck genes (Supplementary Table 1).

Analysis. Results are presented as means ± SEM for the number of hepatocyte isolations indicated. Statistical analysis was by paired *t* test.

RESULTS

Glucose represses Gck concomitantly with induction of Gckr and G6pc. To test the hypothesis that accumulation of phosphorylated intermediates during exposure of hepatocytes to elevated glucose concentration represses Gck gene expression and induces enzymes that deplete the phosphometabolite pool (Fig. 1), hepatocytes were precultured in medium with 5 mmol/L glucose and then incubated for 4 h in medium containing 10 nmol/L insulin and either 5 mmol/L or 25 mmol/L glucose or with an inhibitor of the glucose 6-P translocator (S4048) that enhances the accumulation of glucose 6-P by inhibiting its hydrolysis (21). The rate of glucose phosphorylation was sixfold higher at 25 mmol/L compared with 5 mmol/L glucose and was not affected by S4048, whereas glucose 6-P was increased fivefold by 25 mmol/L glucose and a further fivefold by S4048 (Fig. 2*A*). The mRNA levels of the target genes shown in Fig. 1 were determined in parallel incubation conditions and an additional incubation without insulin (Fig. 2*B*, hatched line). Gck mRNA was markedly increased by insulin, as expected (22), but it was repressed by 25 mmol/L glucose and further repressed by S4048. Expression of Gckr, the inhibitor protein of Gck, was induced by insulin and further induced by glucose. The gluconeogenic enzymes G6pc and Pck1 were both repressed by insulin, but whereas Pck1 was further repressed by 25 mmol/L glucose, G6pc was induced and further elevated by S4048. Expressions of the glycolytic enzyme Pklr and the lipogenic enzyme Fasn were increased by 25 mmol/L glucose and further enhanced by S4048 (Fig. 2*B*). The converse effects of glucose on Gck and Pck1, which catalyze entry of substrate into the phosphometabolite pool as compared with induction of G6pc and Pklr, is consistent with the hypothesis (Fig. 1).

Metabolite accumulation represses Gck. To test for a possible direct effect of glucose on Gck repression, we used the hexokinase inhibitor 5-thioglucose to abolish the elevation in glucose 6-P. Lack of effect of glucose on Gck mRNA in the presence of 5-thioglucose rules out a direct effect of glucose (Fig. 3*A*). To determine whether glucose repression of Gck shows a similar sensitivity to elevated glucose 6-P as Pklr induction, hepatocytes were incubated with S4048 and varying glucose concentration, and Gck and Pklr mRNA were plotted against the respective glucose 6-P (Fig. 3*B*). The mRNA levels of both genes responded sharply over a threefold increase in glucose 6-P above basal with a smaller fractional change at higher metabolite levels and showed a similar sensitivity of response. Insulin induction of liver Gck is mediated by activation of Akt (28). We therefore tested for effects of glucose (+ S4048) on Akt activation. However phosphorylation of Akt was not affected by glucose (+ S4048), indicating that Gck repression is unlikely to be due to attenuated insulin signaling (Fig. 3*C*). Gck mRNA decay was not affected by 25 mmol/L glucose (+ S4048) (Fig. 3*D*), and a comparison of the time course (20–240 min) of Gck-mRNA primary transcript and mature transcript after challenge with insulin showed suppression of both transcripts at 25 mmol/L glucose (+ S4048) (Fig. 3*E*), suggesting repression of transcription.

Glucose-repression of Gck mRNA is dependent on Mlx. Gene microarray studies on hepatocytes using Mlx-DN have demonstrated a major role for Mlx in glucose induction of gene expression but also indicated involvement in gene repression (17). We tested for Mlx involvement in Gck repression by expression of Mlx-DN and Mlx-WT. Appropriate viral titres were determined from expression of Pklr, an established Mlx-ChREBP target (17). Expression of Mlx-DN by sevenfold above endogenous (Fig. 4*A*) counteracted the glucose-induction of Pklr by ~70%, and expression of Mlx-WT (by sevenfold) partially reversed the effect (Fig. 4*A*). Mlx-DN partially counteracted the induction of G6pc and Gckr and also the repression of Gck and Pck1. These effects were partially reversed by Mlx-WT (Fig. 4*A*). The fractional contribution of Mlx to the glucose repression of Gck and Pck1 was lower than for gene induction (Fig. 4*B*).

We also tested the effects of ChREBP-WT and ChREBP-DN on expression of Gck and other target genes. Expression of ChREBP-WT mimicked the glucose-induction of Pklr, G6pc, and Gckr (Fig. 5*A*), and ChREBP-DN attenuated the induction of these genes (Supplementary Fig. 1). However, surprisingly, Gck expression was repressed by both ChREBP-WT (Fig. 5*A*) and ChREBP-DN (Supplementary Fig. 1).

Glucose stimulates recruitment of Mlx to the Gck promoter. We performed ChIP assays to test for direct binding of Mlx and ChREBP to the Gck promoter using

Time course (20–240 min) with insulin at 5 mmol/L glucose or 25 mmol/L glucose + 2 μmol/L S4048. Gck-mRNA: mature transcript (M) and primary transcript (P) expressed relative to time 0. Representative of three experiments. Gck-mRNA primary transcript after 4-h incubation with the additions shown (fold change relative to control without insulin). Means ± SEM, $n = 4$. *$P < 0.05$, effect of insulin; #$P < 0.05$, relative to 5 mmol/L glucose + insulin; ^$P < 0.05$, effect of S4048.

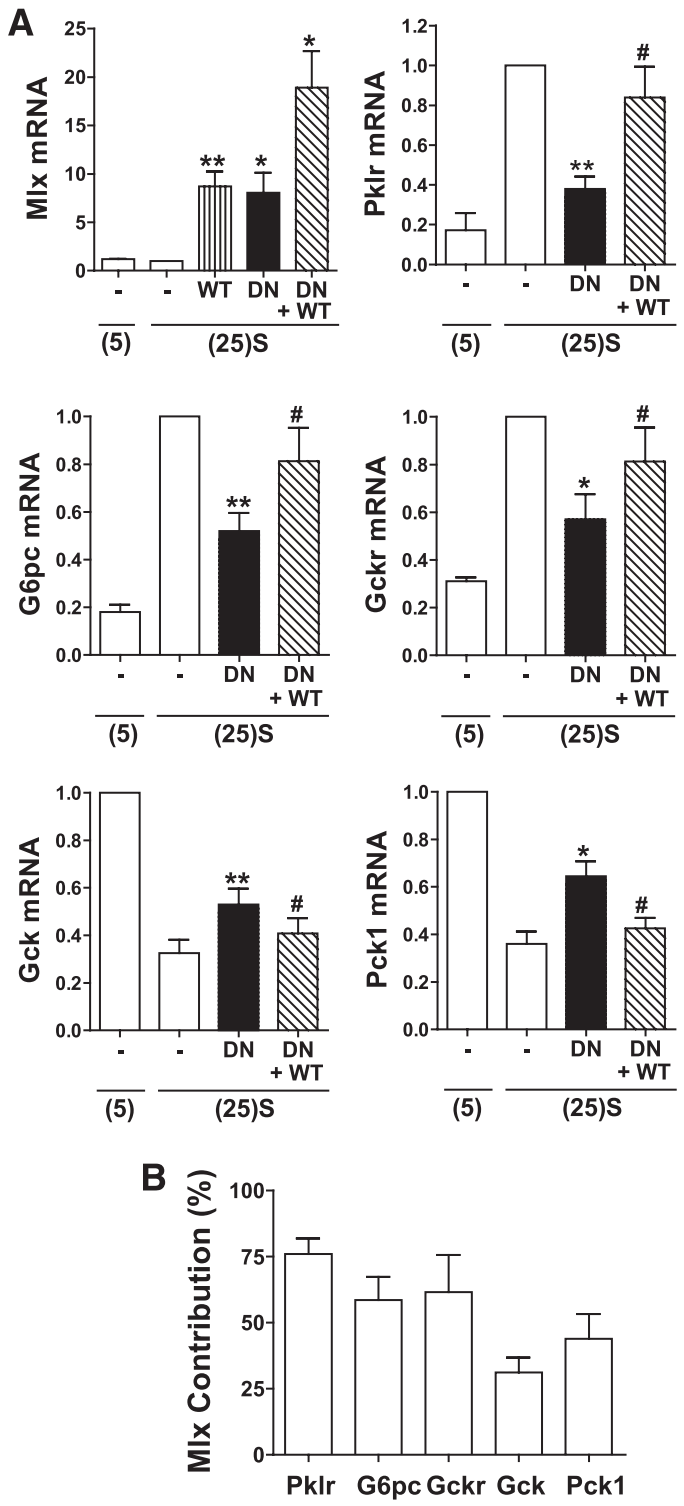

FIG. 4. Involvement of Mlx in the glucose repression of Gck. Hepatocytes were either untreated (open bars) or treated with vectors for expression of Mlx-DN or Mlx-WT. After 18-h preculture they were incubated for 4 h at either 5 mmol/L glucose (5) or 25 mmol/L glucose + 2 μmol/L S4048 [(25)S]. *A*: mRNA levels expressed relative to untreated cells at 25 mmol/L glucose + 2 μmol/L S4048. Means ± SEM, $n = 4$. *$P < 0.05$, **$P < 0.01$, effect of Mlx-DN; #$P < 0.05$, effect of Mlx-WT. *B*: Fractional contribution of Mlx to glucose-regulated gene expression calculated from the Mlx-DN attenuation relative to the glucose response calculated from the data in *A*.

three sets of primers spanning regions from −411 to −25 (29). First, we confirmed that glucose stimulated recruitment of both Mlx and ChREBP to a carbohydrate response element–containing region of the Pklr promoter (Fig. 5*B*), as shown previously in rat insulinoma cells (30). In the same chromatin precipitates, glucose did not affect binding of ChREBP to the Gck promoter using the three primer sets (Fig. 5*C*). However, glucose significantly increased binding of Mlx to the Gck promoter using primers spanning from −145 to −25 but not with primers spanning −411 to −199 and −239 to −111. The −145 to −25 region contains a CACGTG element that binds Mlx heterodimers with transcriptional repressors (31). These results support glucose-dependent binding of Mlx but not ChREBP to the Gck promoter.

Immunoactivity and turnover of Gck and Gckr. We tested for effects of elevated glucose on Gck and Gckr immunoactive protein. No effect was found at 24-h culture (results not shown), but after 48 h, Gckr protein was increased and the Gck-to-Gckr protein ratio was decreased (Fig. 6*A*). The discordance between the rapid changes in mRNA (Fig. 3) and the slow changes in protein could be due to differences in mRNA (22) and protein turnover. Because primary hepatocytes do not permit experiments of longer duration because of dedifferentiation, we assessed turnover of these proteins in vivo using dynamic metabolic labeling (26) by feeding mice a diet containing [$^2H_8$]valine for 35 days, and performed liver proteome analysis at different times (Fig. 6*B*). For Gckr, the peptide **V**IPTALLSLLLR was used to define the rate of turnover, at $0.107 \pm 0.009 d^{-1}$, a half-life of 6.5 days. Gck had a lower abundance than Gckr, and even the most intense peptides (ASGAEGNNI**V**GLLR and LETHQEAS**V**K) gave less intense signals, leading to greater noise in the labeling curve. Nonetheless, the fitted first-order curve yielded a rate constant of $0.15 \pm 0.008\ d^{-1}$, a half-life of 4.6 days. Given that the half-life of mouse liver protein is less than a day, both Gck and Gckr would be classified as low turnover. Moreover the rate of protein turnover in rats (and humans) would be substantially lower than in the mouse. Consequently, changes in protein expression in vivo would only be expected after chronic exposure.

Metabolite homeostasis in hepatocytes is dependent on Gck and G6pc activity. The hypothesis (Fig. 1) predicts that elevated Gck activity and/or decreased G6pc activity compromises metabolite homeostasis. Depletion of ATP in insulinoma cells during twenty-fold overexpression of Gck has been demonstrated (32). We tested whether titrated overexpression of Gck by 70% to fourfold above endogenous, affects ATP and glucose 6-P homeostasis when combined with G6pc inhibition with S4048. At endogenous Gck, challenge with 25 mmol/L glucose for 4 h did not affect cell ATP, whereas fructose lowered ATP by 32% between 30 and 60 min ($P < 0.002$) (Fig. 7*A*). Overexpression of Gck by threefold or inhibition of G6pc activity with S4048 lowered ATP (15–20% at 30–60 min $P < 0.001$), whereas combined S4048 and Gck overexpression caused more severe ATP depletion (65% at 30 min, $P < 0.001$). Interestingly, the decline in ATP was partially reversed by 240 min, despite sustained elevation of glucose 6-P (Fig. 7*B*). Perturbation of the activity of a single enzyme is predicted to cause larger changes in metabolite concentration than in metabolic flux (33). We confirmed that this is the case for Gck by comparing the effects of Gck overexpression on glucose phosphorylation, glucose 6-P accumulation, and ATP depletion (Fig. 7*C–E*). Response coefficients represented by the slopes

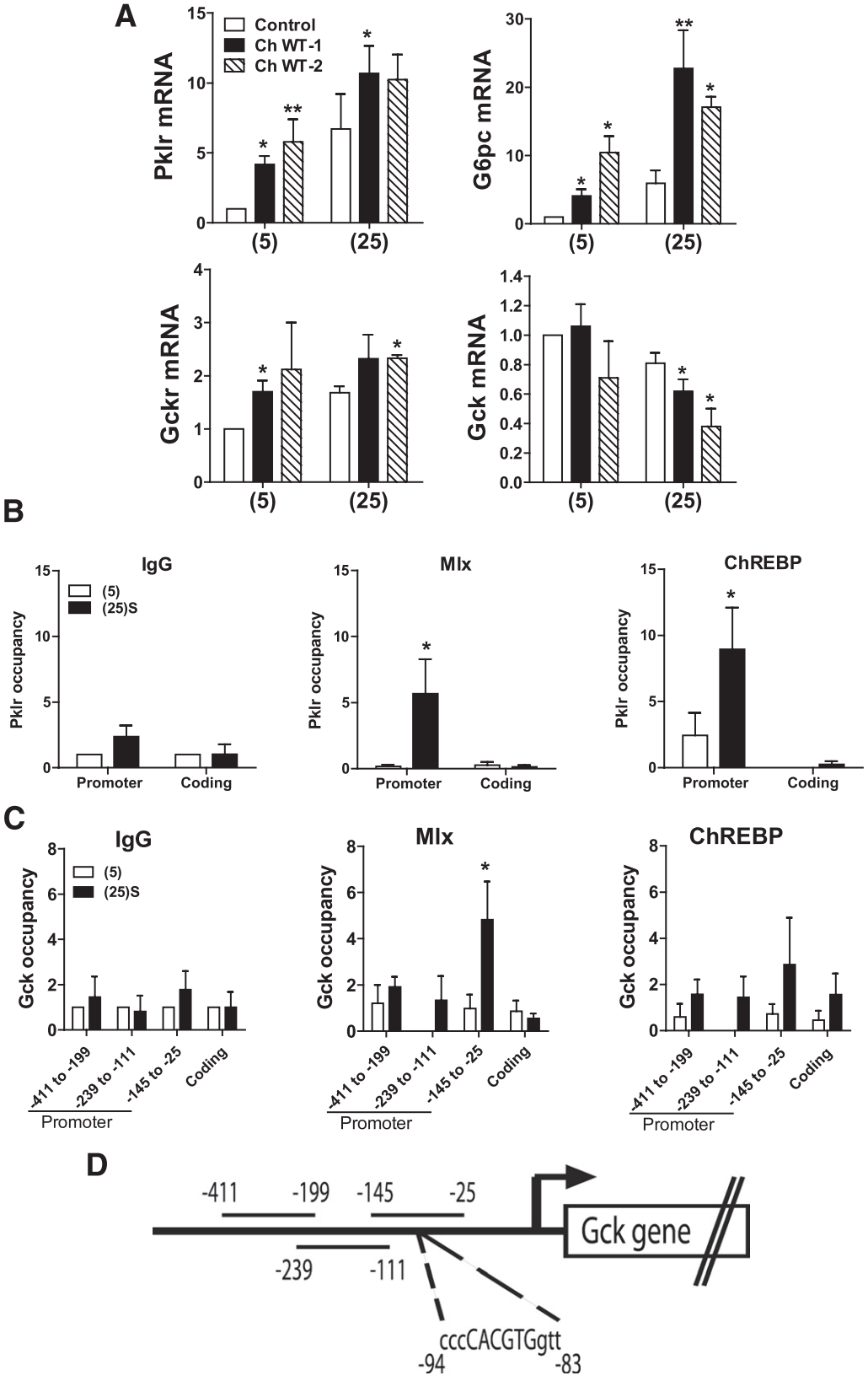

FIG. 5. Glucose-dependent binding of Mlx to the Gck promoter. *A*: Effects of overexpression of ChREBP-WT on Pklr, G6pc, Gckr, and Gck mRNA expression. Hepatocytes were either untreated (open bars) or treated with vectors for expression of ChREBP-WT at two viral titres (twofold dilution). After 18-h preculture, they were incubated for 4 h with 5 mmol/L (5) or 25 mmol/L (25) glucose. mRNA levels are expressed relative to untreated at 5 mmol/L glucose. Means ± SEM, $n = 4$–10. *$P < 0.05$, **$P < 0.001$, effect of ChREBP-WT. *B* and *C*: Recruitment of Mlx and ChREBP to the Pklr promoter and the Gck promoter. Hepatocytes were incubated for 4 h with 5 mmol/L glucose or 25 mmol/L glucose + 2 μmol/L S4048 [(25)S]. Chromatin immunoprecipitation was performed as described in RESEARCH DESIGN AND METHODS using either control IgG, or antibody to Mlx or ChREBP. The promoter and coding regions of the Pklr (*B*) and Gck (*C*) genes were amplified by real-time RT-PCR and binding of Mlx and ChREBP is expressed relative to the IgG control at 5 mmol/L glucose. For Pklr, the carbohydrate response element–containing region (30) of the promoter was amplified. For Gck, three regions of the promoter (29) spanning the residues indicated (*D*) were amplified. Results are means ± SEM, $n = 4$. *$P < 0.05$ relative to 5 mmol/L glucose.

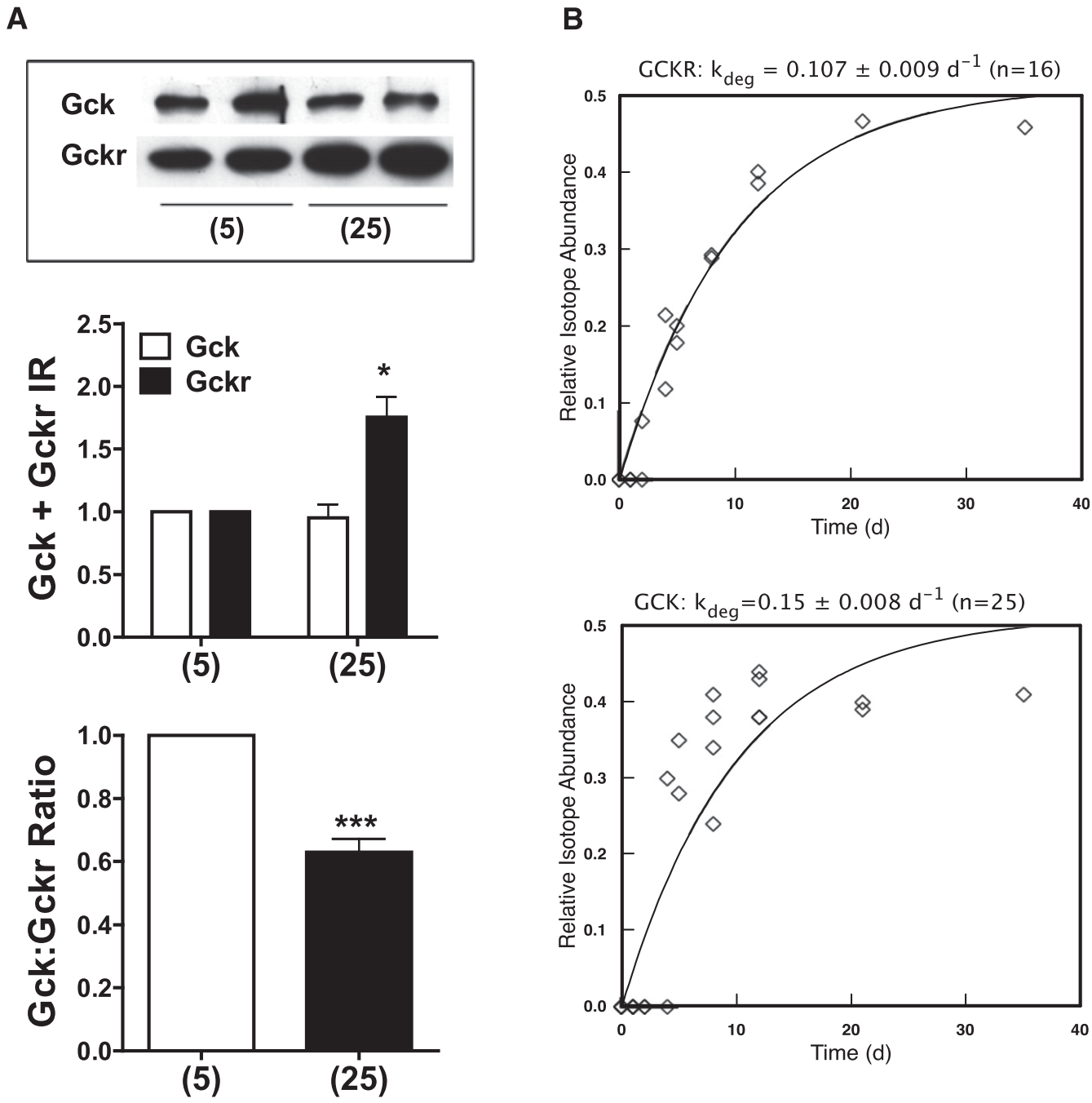

FIG. 6. Gck and Gckr immunoactivity in hepatocytes and protein turnover in vivo. *A*: Rat hepatocytes were cultured for 48 h with the substrates indicated and immunoactivity to Gck and Gckr was determined by immunoblotting and quantified by densitometry. Results are means ± SEM, $n = 4$. *$P < 0.05$, ***$P < 0.005$ relative to 5 mmol/L glucose. *B*: Turnover of Gck and Gckr in vivo in mice fed a diet containing [$^2H_8$]valine at a relative abundance of 0.5. As proteins become labeled, the valine in peptides approaches the precursor monoexponentially. The delay in labeling at day (d) 1–2 reflects equilibration of the body pools with the ingested label and does not influence the estimate of the rate constant. Turnover was calculated by nonlinear curve-fitting of the labeling curve. Gckr: half-life 6.5 days; Gck half-life, 4.6 days.

of double log plots (Fig. 7*F*) were higher for glucose 6-P (1.56, 1.48) than for glucose phosphorylation flux (0.97, 0.53). ATP determined at 60 min declined with Gck expression or G6pc inhibition (Fig. 7*E*) and correlated inversely with glucose 6-P (Fig. 7*G*; r −0.963, $P < 0.0001$), confirming coordinate roles for G6pc and Gck in metabolite homeostasis.

Uric acid production by hepatocytes is dependent on glucose metabolism. The transient decline in ATP despite sustained elevation in glucose 6-P (Fig. 7*A* and *B*) is most likely due to a transient decline in cell inorganic phosphate (Pi), as occurs with fructose loading (34–36). To test for this possibility, we determined uric acid formation as an index of cytoplasmic Pi depletion. Uric acid is the end product of purine degradation in the human liver (Fig. 8*A*). Degradation of adenine nucleotides to uric acid involves conversion of AMP to inosine monophosphate by AMP deaminase, which is allosterically inhibited by physiological concentrations of Pi (37). The enzyme is activated by Pi depletion (37), and consequently uric acid production is a sensitive index of cell Pi depletion (38–40). Because

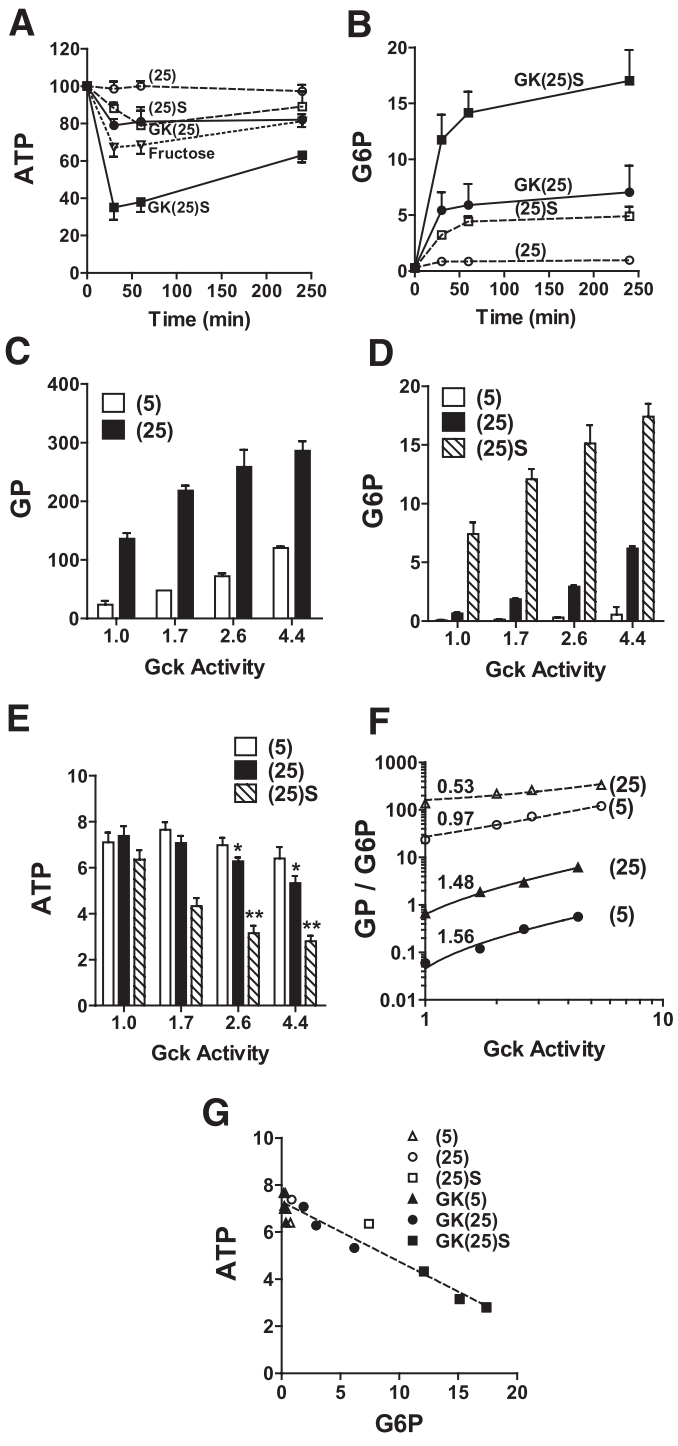

FIG. 7. Overexpression of Gck compromises hepatocyte glucose 6-P and ATP homeostasis. Hepatocytes were untreated or treated with three titres of adenoviral vector for expression of Gck (by 1.7–4.4 fold relative to endogenous Gck activity) and cultured for 18 h in MEM containing 5 mmol/L glucose as described in RESEARCH DESIGN AND METHODS. *A* and *B*: Time course of hepatocyte ATP and glucose 6-P in untreated hepatocytes (open symbols) or cells with fourfold Gck overexpression (filled symbols) incubated in MEM containing 25 mmol/L glucose without (25) or with 2 μmol/L S4048 [(25)S] or with 5 mmol/L fructose (open triangle). *C–E*: Rates of glucose phosphorylation (metabolism of [2-^{3}H]glucose) and cell glucose 6-P and ATP determined after 60-min incubation with 5 mmol/L or 25 mmol/L glucose without or with 2 μmol/L S4048, in hepatocytes expressing endogenous Gck (1) or 1.7–4.4 Gck overexpression. Means ± SEM, $n = 4$. *$P < 0.05$; **$P < 0.005$ relative to corresponding ATP values at endogenous Gck activity. *F*: Double log plot of glucose phosphorylation (open symbols) or glucose 6-P (filled symbols) vs. corresponding Gck activity (data from *C* and *D*). *G*: ATP vs. glucose 6-P (data from *D* and *E*).

uric acid is further metabolized by uric acid oxidase to S-allantoin in rat hepatocytes (Fig. 8*A*), we used oxonic acid, an inhibitor of uric acid oxidase, to measure uric acid formation. Oxonic acid caused concentration-dependent inhibition of degradation of exogenous uric acid (Fig. 8*B*), and it increased endogenous uric acid accumulation during incubation of hepatocytes with fructose (Fig. 8*C*). In the presence of 0.5 mmol/L oxonic acid, the basal rate of uric acid production was stimulated by fructose in a concentration-dependent manner and to a lesser extent by 25–35 mmol/L glucose (Fig. 8*D*). In the presence of 25 mmol/L glucose (Fig. 8*E*), uric acid production was enhanced by Gck overexpression and attenuated by Gckr overexpression, consistent with an effect of the Gck-to-Gckr ratio on cell Pi homeostasis.

DISCUSSION

A defect in Gck expression or regulation has been blamed for the reduced hepatic glucose uptake in type 2 diabetes (8–10). Liver Gck activity is markedly suppressed in animal models of diabetes, including the insulin-deficient streptozotocin model and the insulin-resistant ZDF rat (41,42), and this defect is either partially (41) or totally reversed (42) by correction of the hyperglycemia with long-term treatment for 2–4 weeks with inhibitors of renal glucose reabsorption (phlorizin or T-1095). However, a direct effect of glucose on hepatic Gck expression has to our knowledge neither been invoked nor demonstrated (5). Insulin and glucagon are major regulators of Gck expression (5), and impaired Gck expression in diabetes is generally attributed to defects in insulin secretion or action (42). Studies in vivo cannot distinguish between direct regulation by glucose and endocrine control. Consequently, the question whether hyperglycemia per se through a direct effect of glucose on the hepatocyte as distinct from changes in insulin sensitivity is a factor in the Gck defect in diabetes remains unsettled.

In this study, we tested the hypothesis that high glucose represses the Gck gene through a direct effect on the hepatocyte and concomitantly with the induction of G6pc (13–16), and that this mechanism serves to preserve cell phosphate homeostasis. We provide three sets of evidence in support of this hypothesis. First, we demonstrate that Gck is repressed by glucose at the mRNA level concomitantly with the induction of G6pc. Secondly, we show that S4048, an inhibitor of the glucose 6-P transporter, that causes marked elevation of glucose 6-P, potentiates the glucose-induction of G6pc and the repression of Gck. Because S4048 has negligible effect on glucose phosphorylation flux (Fig. 2), this supports a mechanism triggered by metabolite accumulation rather than metabolic flux. An effect of S4048 on Gck mRNA repression in vivo has been demonstrated (43,44). However, since S4048 causes acute hypoglycemia, these in vivo studies could not resolve the effects of metabolite accumulation from secondary endocrine changes induced by hypoglycemia. Thirdly, we show that although insulin induces both Gck and its inhibitor protein, Gckr, glucose has converse effects on Gck (repression) and Gckr (induction) with a consequent decrease in the Gck-to-Gckr ratio at both the mRNA (at 4 h) and protein (after 48 h) levels. Previous studies have shown that both Gck and Gckr have very high control strengths on hepatic glucose metabolism and that small fractional changes in either protein have a major influence on hepatic glucose disposal (2–4). Thus, a decrease in the

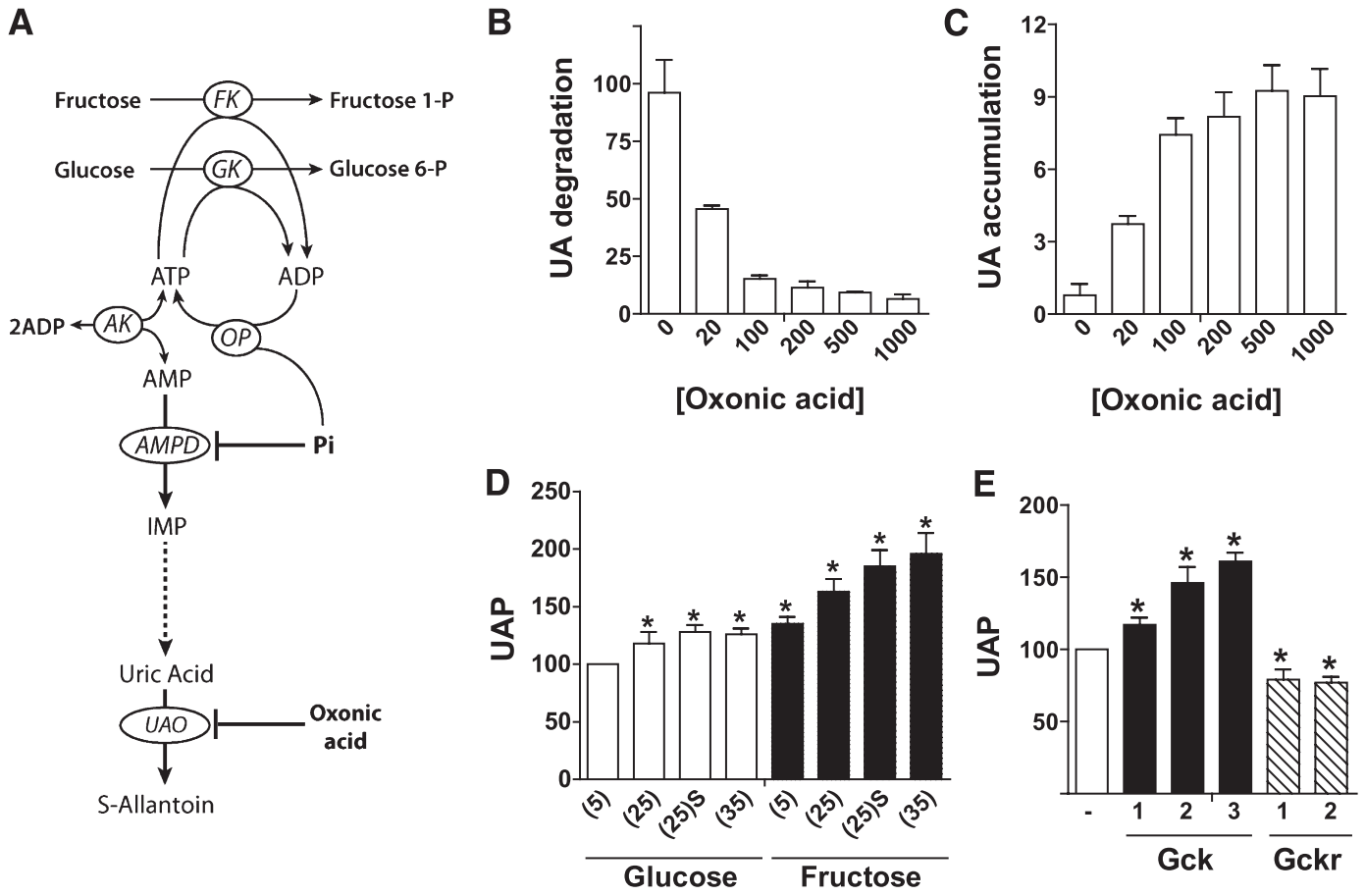

FIG. 8. Glucose metabolism affects uric acid production by hepatocytes. *A*: Uric acid is the final product of purine degradation in humans because of lack of a functional urate oxidase (UAO) gene. In other mammals, uric acid is further metabolized to S-allantoin by urate oxidase. AMP-deaminase (AMPD) catalyses the conversion of AMP to inosine monophosphate and is inhibited by physiological concentrations of Pi. During ATP-dependent phosphorylation of fructose or glucose, the ADP generated at the level of fructokinase (FK) or glucokinase (GK) is reconverted to ATP by oxidative phosphorylation (OP). If accumulation of phosphorylated intermediates during sugar metabolism causes depletion of Pi, then AMPD is deinhibited, resulting in degradation of AMP to uric acid. *B*: Oxonic acid inhibits uric acid degradation. Rat hepatocytes were incubated for 30 or 60 min in medium containing 100 μmol/L uric acid and the concentrations of oxonic acid (μmol/L) shown. Uric degradation is expressed as nmol/h per mg protein. *C*: Effects of oxonic acid on uric acid accumulation in the medium (nmol/h per mg) during incubation of hepatocytes in medium containing 30 mmol/L fructose and the oxonic acid concentrations (μmol/L) indicated. *D*: Effects of glucose and fructose on uric acid production (UAP, expressed as % control) in hepatocytes incubated for 1 h in medium containing 500 μmol/L oxonic acid and the substrates indicated (5, 25, or 35 mmol/L substrate or 25 mmol/L substrate + S4048 [(25)S]). *E*: Uric acid production (expressed as % control) in hepatocytes treated with adenoviral vectors for overexpression of Gck (2.5 to 10-fold) or Gckr (four- to sixfold) and incubated for 1 h in medium containing 25 mmol/L glucose. Means ± SEM, $n = 3$ (*B* and *C*); $n = 3$–7 (*D* and *E*). *$P < 0.05$ relative to 5 mmol/L glucose (*D*) or relative to untreated (*E*).

hepatic Gck-to-Gckr protein ratio induced by elevated glucose is predicted to cause a rightward shift in the hepatic response to glucose concentration (1), providing an explanation for the defect in glucose uptake in type 2 diabetes (10). We show that changes in the Gck-to-Gckr protein ratio are much slower than mRNA changes but also that both Gck and Gckr are low-turnover proteins. Moreover, the rate of protein turnover in the rat, and more so in humans, would be substantially lower than in the mouse. Thus, glucose regulation of the Gck-to-Gckr ratio would be expected to occur following chronic rather than acute exposure to hyperglycemia. Direct evidence for a pathological role for this mechanism therefore poses a major challenge. Nonetheless, it is accepted that induction of glycolytic (Pklr) and lipogenic genes (Fasn) by glucose via Mlx-ChREBP is a major contributing factor to fatty liver (17). The apparent similar sensitivity of Gck repression and Pklr induction to metabolite accumulation suggests that these mechanisms would be activated in similar pathophysiological states and, accordingly, that impaired glucose tolerance and fatty liver may share the same triggering stimuli. However, despite the similar sensitivity to metabolite accumulation between Gck repression and Pklr induction (Fig. 3*B*), our study provides evidence, based on expression studies with Mlx-DN and chromatin immunoprecipitation assays, for involvement of Mlx but not ChREBP in glucose repression of Gck. The latter showed that glucose caused the recruitment of Mlx to the Gck promoter using primers spanning the −145 to −25. This region contains a CACGTG element that binds Mlx heterodimers with transcriptional repressors of the Mad family (Mxd1 and Mxd4) and Mnt (31). Identification of the Mlx partner and the mechanism(s) that links glucose metabolism with recruitment of Mlx to the Gck promoter is important to understanding Gck regulation in diabetes.

Induction of G6pc and elevation in the Gckr-to-Gck ratio by elevated glucose protects against excessive accumulation of phosphorylated intermediates of glucose metabolism. The hepatic concentration of glucose 6-P is approximately

twofold higher in the ad libitum–fed state compared with the fasted state (45). However, a high-carbohydrate meal after a 48-h fast causes a far greater elevation in metabolic intermediates (45). Chronic meal feeding may enable adaptive regulation of gene expression to buffer metabolite accumulation. A key consequence of rapid accumulation of phosphorylated intermediates is the acute depletion of Pi (34–37), resulting in degradation of adenine nucleotides to uric acid (37–40). Two metabolic situations in which severe Pi imbalance occurs in humans are fructose loading (34,36,38,39) and deficiency of G6pc in glycogen storage disease type 1 (46). Both are characterized by depletion of liver ATP and elevated uric acid production. We show that moderate overexpression of Gck in hepatocytes above endogenous levels causes ATP depletion and enhanced uric acid production at elevated glucose. Inhibition of G6pc with S4048 further enhances these effects, confirming the role of G6pc in buffering the concentrations of phosphorylated intermediates. The attenuation of uric acid production by Gckr overexpression indicates a protective role of this Gck inhibitor in preserving homeostasis of phosphorylated metabolites. These results provide a potential explanation for the recent demonstration of an association between an intronic single nucleotide polymorphism (rs780094) in the Gckr gene and elevated serum urate levels (47,48). The minor T-allele is associated with lower fasting glucose and raised triglycerides and uric acid levels. The low glucose and high triglyceride predicts increased Gck activity, and the elevated urate is consistent with the present finding that endogenous urate production by hepatocytes is influenced by the Gck-to-Gckr ratio.

ACKNOWLEDGMENTS

This work was supported by a Research Grant from the Medical Research Council (G0501543) and by Equipment Grant support from Diabetes UK (07/0003488). J.L.P. was supported by a Diabetes UK research studentship (07/003559).

No potential conflicts of interest relevant to this article were reported.

C.A., J.L.P., S.J.T., and Z.A.-O. researched data, contributed to discussion, and reviewed and edited the manuscript. A.J.C. researched data. R.J.B. researched data and contributed to discussion. H.C.T. contributed to discussion and reviewed and edited the manuscript. L.A. directed the study and wrote the manuscript.

The authors thank Professor Philip Home, Institute of Cellular Medicine, Newcastle University, Newcastle upon Tyne, U.K., for encouragement and support.

REFERENCES

1. Agius L. Glucokinase and molecular aspects of liver glycogen metabolism. Biochem J 2008;414:1–18
2. Agius L, Peak M, Newgard CB, Gomez-Foix AM, Guinovart JJ. Evidence for a role of glucose-induced translocation of glucokinase in the control of hepatic glycogen synthesis. J Biol Chem 1996;271:30479–30486
3. Van Schaftingen E. Glycolysis revisited. Diabetologia 1993;36:581–588
4. de la Iglesia N, Mukhtar M, Seoane J, Guinovart JJ, Agius L. The role of the regulatory protein of glucokinase in the glucose sensory mechanism of the hepatocyte. J Biol Chem 2000;275:10597–10603
5. Iynedjian PB. Molecular physiology of mammalian glucokinase. Cell Mol Life Sci 2009;66:27–42
6. Mevorach M, Giacca A, Aharon Y, Hawkins M, Shamoon H, Rossetti L. Regulation of endogenous glucose production by glucose per se is impaired in type 2 diabetes mellitus. J Clin Invest 1998;102:744–753
7. Hawkins M, Gabriely I, Wozniak R, Reddy K, Rossetti L, Shamoon H. Glycemic control determines hepatic and peripheral glucose effectiveness in type 2 diabetic subjects. Diabetes 2002;51:2179–2189
8. Basu A, Basu R, Shah P, et al. Effects of type 2 diabetes on the ability of insulin and glucose to regulate splanchnic and muscle glucose metabolism: evidence for a defect in hepatic glucokinase activity. Diabetes 2000;49:272–283
9. Basu A, Basu R, Shah P, et al. Type 2 diabetes impairs splanchnic uptake of glucose but does not alter intestinal glucose absorption during enteral glucose feeding: additional evidence for a defect in hepatic glucokinase activity. Diabetes 2001;50:1351–1362
10. Rizza RA. Pathogenesis of fasting and postprandial hyperglycemia in type 2 diabetes: implications for therapy. Diabetes 2010;59:2697–2707
11. Seoane J, Trinh K, O'Doherty RM, et al. Metabolic impact of adenovirus-mediated overexpression of the glucose-6-phosphatase catalytic subunit in hepatocytes. J Biol Chem 1997;272:26972–26977
12. Aiston S, Trinh KY, Lange AJ, Newgard CB, Agius L. Glucose-6-phosphatase overexpression lowers glucose 6-phosphate and inhibits glycogen synthesis and glycolysis in hepatocytes without affecting glucokinase translocation. Evidence against feedback inhibition of glucokinase. J Biol Chem 1999;274:24559–24566
13. Massillon D, Barzilai N, Chen W, Hu M, Rossetti L. Glucose regulates in vivo glucose-6-phosphatase gene expression in the liver of diabetic rats. J Biol Chem 1996;271:9871–9874
14. Argaud D, Kirby TL, Newgard CB, Lange AJ. Stimulation of glucose-6-phosphatase gene expression by glucose and fructose-2,6-bisphosphate. J Biol Chem 1997;272:12854–12861
15. Massillon D. Regulation of the glucose-6-phosphatase gene by glucose occurs by transcriptional and post-transcriptional mechanisms. Differential effect of glucose and xylitol. J Biol Chem 2001;276:4055–4062
16. Pedersen KB, Zhang P, Doumen C, et al. The promoter for the gene encoding the catalytic subunit of rat glucose-6-phosphatase contains two distinct glucose-responsive regions. Am J Physiol Endocrinol Metab 2007;292:E788–E801
17. Ma L, Robinson LN, Towle HC. ChREBP*Mlx is the principal mediator of glucose-induced gene expression in the liver. J Biol Chem 2006;281:28721–28730
18. Hutton JC, O'Brien RM. Glucose-6-phosphatase catalytic subunit gene family. J Biol Chem 2009;284:29241–29245
19. Nordlie RC, Foster JD. A retrospective review of the roles of multifunctional glucose-6-phosphatase in blood glucose homeostasis: Genesis of the tuning/retuning hypothesis. Life Sci 2010;87:339–349
20. Scott DK, O'Doherty RM, Stafford JM, Newgard CB, Granner DK. The repression of hormone-activated PEPCK gene expression by glucose is insulin-independent but requires glucose metabolism. J Biol Chem 1998;273:24145–24151
21. Härndahl L, Schmoll D, Herling AW, Agius L. The role of glucose 6-phosphate in mediating the effects of glucokinase overexpression on hepatic glucose metabolism. FEBS J 2006;273:336–346
22. Iynedjian PB, Jotterand D, Nouspikel T, Asfari M, Pilot PR. Transcriptional induction of glucokinase gene by insulin in cultured liver cells and its repression by the glucagon-cAMP system. J Biol Chem 1989;264:21824–21829
23. Zhu A, Romero R, Petty HR. An enzymatic fluorimetric assay for glucose-6-phosphate: application in an in vitro Warburg-like effect. Anal Biochem 2009;388:97–101
24. Benzie IF, Strain JJ. The ferric reducing ability of plasma (FRAP) as a measure of "antioxidant power": the FRAP assay. Anal Biochem 1996;239:70–76
25. Trivedi RC, Rebar L, Berta E, Stong L. New enzymatic method for serum uric acid at 500 nm. Clin Chem 1978;24:1908–1911
26. Doherty MK, Whitehead C, McCormack H, Gaskell SJ, Beynon RJ. Proteome dynamics in complex organisms: using stable isotopes to monitor individual protein turnover rates. Proteomics 2005;5:522–533
27. Arden C, Hampson LJ, Huang GC, et al. A role for PFK-2/FBPase-2, as distinct from fructose 2,6-bisphosphate, in regulation of insulin secretion in pancreatic beta-cells. Biochem J 2008;411:41–51
28. Iynedjian PB, Roth RA, Fleischmann M, Gjinovci A. Activation of protein kinase B/cAkt in hepatocytes is sufficient for the induction of expression of the gene encoding glucokinase. Biochem J 2000;351:621–627
29. Magnuson MA, Andreone TL, Printz RL, Koch S, Granner DK. Rat glucokinase gene: structure and regulation by insulin. Proc Natl Acad Sci USA 1989;86:4838–4842
30. Burke SJ, Collier JJ, Scott DK. cAMP opposes the glucose-mediated induction of the L-PK gene by preventing the recruitment of a complex containing ChREBP, HNF4alpha, and CBP. FASEB J 2009;23:2855–2865

31. Billin AN, Eilers AL, Queva C, Ayer DE. Mlx, a novel Max-like BHLHZip protein that interacts with the Max network of transcription factors. J Biol Chem 1999;274:36344–36350
32. Wang H, Iynedjian PB. Acute glucose intolerance in insulinoma cells with unbalanced overexpression of glucokinase. J Biol Chem 1997;272:25731–25736
33. Raamsdonk LM, Teusink B, Broadhurst D, et al. A functional genomics strategy that uses metabolome data to reveal the phenotype of silent mutations. Nat Biotechnol 2001;19:45–50
34. Mayes PA. Intermediary metabolism of fructose. Am J Clin Nutr 1993;58 (Suppl.):754S–765S
35. Woods HF, Krebs HA. Xylitol metabolism in the isolated perfused rat liver. Biochem J 1973;134:437–443
36. Masson S, Henriksen O, Stengaard A, Thomsen C, Quistorff B. Hepatic metabolism during constant infusion of fructose; comparative studies with ^{31}P-magnetic resonance spectroscopy in man and rats. Biochim Biophys Acta 1994;1199:166–174
37. van den Berghe G, Bronfman M, Vanneste R, Hers HG. The mechanism of adenosine triphosphate depletion in the liver after a load of fructose. A kinetic study of liver adenylate deaminase. Biochem J 1977;162:601–609
38. Perheentupa J, Raivio K. Fructose-induced hyperuricaemia. Lancet 1967;2: 528–531
39. Mäenpää PH, Raivio KO, Kekomäki MP. Liver adenine nucleotides: fructose-induced depletion and its effect on protein synthesis. Science 1968;161:1253–1254
40. Morris RC Jr, Nigon K, Reed EB. Evidence that the severity of depletion of inorganic phosphate determines the severity of the disturbance of adenine nucleotide metabolism in the liver and renal cortex of the fructose-loaded rat. J Clin Invest 1978;61:209–220
41. Brichard SM, Henquin JC, Girard J. Phlorizin treatment of diabetic rats partially reverses the abnormal expression of genes involved in hepatic glucose metabolism. Diabetologia 1993;36:292–298
42. Nawano M, Oku A, Ueta K, et al. Hyperglycemia contributes insulin resistance in hepatic and adipose tissue but not skeletal muscle of ZDF rats. Am J Physiol Endocrinol Metab 2000;278:E535–E543
43. van Dijk TH, van der Sluijs FH, Wiegman CH, et al. Acute inhibition of hepatic glucose-6-phosphatase does not affect gluconeogenesis but directs gluconeogenic flux toward glycogen in fasted rats. A pharmacological study with the chlorogenic acid derivative S4048. J Biol Chem 2001;276: 25727–25735
44. Grefhorst A, Schreurs M, Oosterveer MH, et al. Carbohydrate-response-element-binding protein (ChREBP) and not the liver X receptor α (LXRα) mediates elevated hepatic lipogenic gene expression in a mouse model of glycogen storage disease type 1. Biochem J 2010;432:249–254
45. Casazza JP, Veech RL. The content of pentose-cycle intermediates in liver in starved, fed ad libitum and meal-fed rats. Biochem J 1986;236: 635–641
46. Greene HL, Wilson FA, Hefferan P, et al. ATP depletion, a possible role in the pathogenesis of hyperuricemia in glycogen storage disease type I. J Clin Invest 1978;62:321–328
47. Kolz M, Johnson T, Sanna S, et al.; EUROSPAN Consortium; ENGAGE Consortium; PROCARDIS Consortium; KORA Study; WTCCC. Meta-analysis of 28,141 individuals identifies common variants within five new loci that influence uric acid concentrations. PLoS Genet 2009;5: e1000504
48. van der Harst P, Bakker SJ, de Boer RA, et al. Replication of the five novel loci for uric acid concentrations and potential mediating mechanisms. Hum Mol Genet 2010;19:387–395